Journal of Physics: Conference Series **530** (2014) 012058 doi:10.1088/1742-6596/530/1/012058

PIV measurements of interface turbulence over hetero-porous media

T Iida, A Taneo, M Kaneda and K Suga
Department of Mechanical Engineering, Osaka Prefecture University, Sakai, Osaka 599-8531, Japan

E-mail: iida@htlab.me.osakafu-u.ac.jp

Abstract. In order to understand turbulent flow physics in the interface region over porous media, PIV measurements are carried out by the refractive index matching method. Two kinds of heterogeneous model porous media, whose porosities are the same but mean pore diameters are different, are applied to the measurements. The turbulent flow fields are discussed using the statistical measurement data. It is found that the fluctuation velocities increase as the mean pore diameter increases inside porous media. Also, it is confirmed that the fluctuation velocity normal to the interface increases as the interface-normal permeability increases.

1. Introduction

Understanding turbulent flow physics near highly porous materials is important for designing industrial devices such as catalyst converters, heat exchangers and flow channels inside fuel cells. Accordingly, many research studies including the authors' group's [1-3] have been carried out for turbulence over porous media. However, turbulence structure in the interface region and the effects of porous structures on turbulence are still not well understood. Furthermore, the effects of heterogeneity of the porous medium structure on turbulence are unknown. Thus, PIV measurements are carried out by the refractive index matching method using water and fluorinated ethylene-propylene (FEP) copolymer in this study. Two kinds of heterogeneous model porous media are applied to the measurements.

2. Experimental methods and procedures

2.1. Experimental setup and porous media

Figure 1 shows the experimental setup. Tap water is collected in the tank, and the water is pumped up from the tank. The flow gets through a digital flow meter and conditioned by a honeycomb section where its temperature is recorded by a digital thermometer. Then the flow is introduced into the test section that is made of transparent acrylic resin. Figure 2 shows the test section. The length of the test section is 1000mm and the width and the height are 50mm and 100mm, respectively. In the test section handmade porous medium blocks are settled up to the bottom half of the duct height. The porous media applied are made of FEP tubes or polypropylene tubes whose diameter is 3mm. FEP is a kind of fluorocarbon resin whose refractive index is 1.34 that is about the same as that of water (1.33). Thus, it allows us to access optically inside the porous media without refractive skewness. The two hetero-porous media have the same porosity and similar permeabilities but the mean pore diameters are different as shown in table 1. The structures of porous media are shown in figure 3. The difference

between type A and type B is the setting angle of the *y*-direction tubes. The setting angle of type A is 45° while that of type B is 60° as shown in figure 3. Following the method applied in [1], the permeabilities are measured using the channel flow facility whose length is 1000mm and the width and height are both 50mm. In between the pressure holes, the porous media were placed to block the flow. The flow rate Q and the pressure drop $\Delta P/\Delta x$ along the porous media were respectively measured by a digital flow meter (FD-MH50A, KEYENCE) and a differential pressure gauge (AP12S, KEYENCE), respectively. With those variables at several different conditions, the permeability and the Forchheimer coefficient can be obtained using the Darcy-Forchheimer equation,

$$-\frac{\Delta P}{\Delta x} = \frac{\mu U_d}{K} + \frac{c_F}{\sqrt{K}} \rho U_d^2 \tag{1}$$

where μ, ρ, K, c_F and U_d are the fluid viscosity, density, the permeability, the Forchheimer coefficient and the mean velocity which can be obtained from Q, respectively. The mean pore diameter D_p is calculated from the volume of spheroid which is circumscribed by the tubes composing the porous medium by using the Sauter mean diameter method.

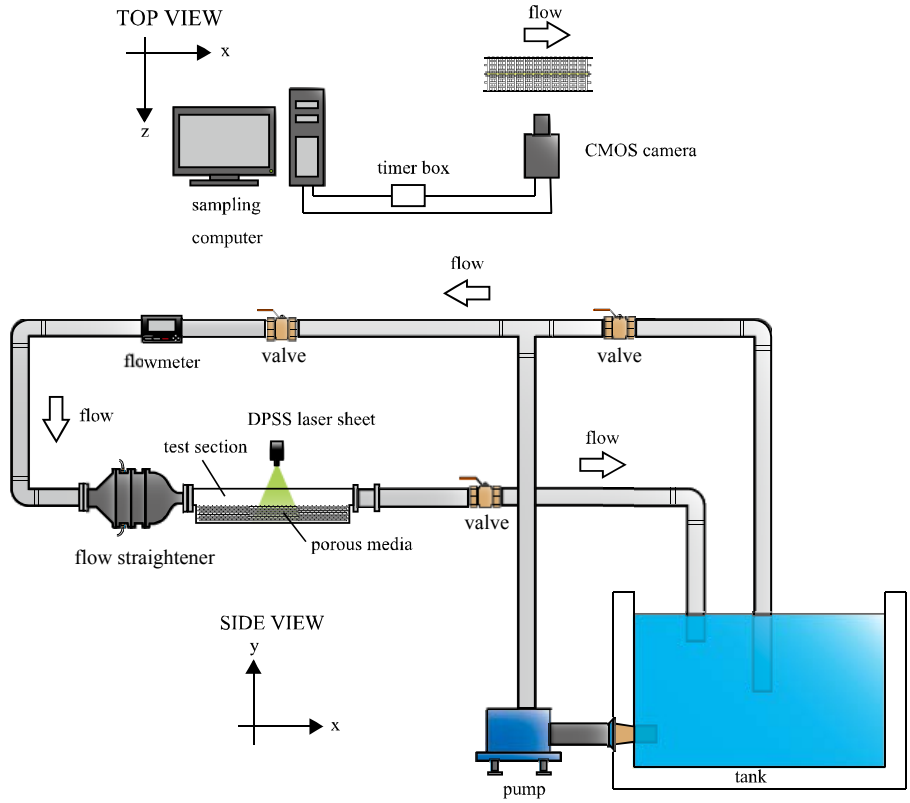

Figure 1. Experimental setup.

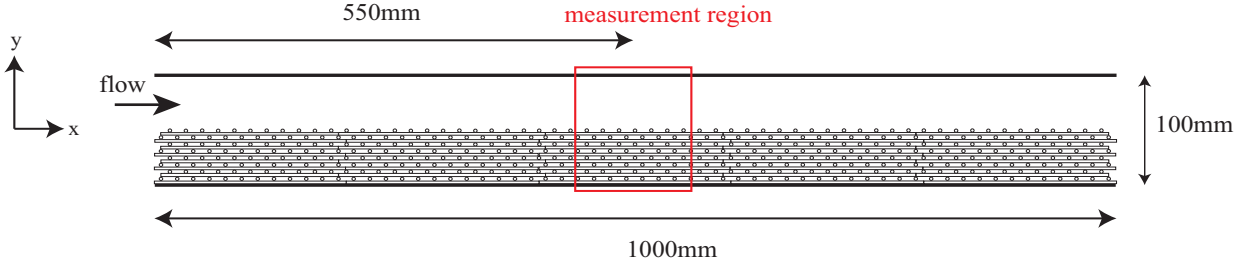

Figure 2. Test section.

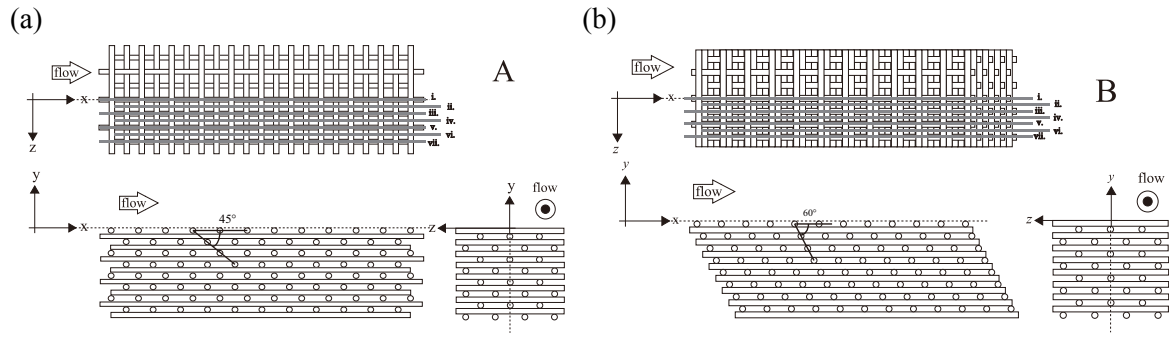

Figure 3. Porous media; (a)type A, (b)type B.

Table 1. Characteristics of porous media.

porous media	porosity φ	streamwise permeability K_x[mm^2]	cross-streamwise permeability K_y[mm^2]	absolute value of permeability K[mm^2]	mean pore diameter D_p[mm]
type A	0.8	0.32	0.25	0.41	8
type B	0.8	0.27	0.26	0.37	12

2.2. PIV measurements

The measurement procedure follows [4]. The measuring area is located at the 550mm distance from the inlet of the test section as shown in figure 2. The PIV system consists of a double-pulse diode pumped solid state (DPSS) laser with the frequency of 532nm (Ray Power 2000, DANTEC DYNAMICS), a high speed complementary metal-oxide-semiconductor (CMOS) camera (Speed Sense 9040, PHANTOM), a camera lens (MICRO-NIKKOR 55 mm f/2.8D), a sharp cut filter (SCF-50S-56O, SIGMAKOKI) and a computer for the data analysis. The laser light is expanded to a sheet light with about 1.0mm thickness and illuminates the measuring sections of the measuring area where the instantaneous images of 1623×1200 pixels are recorded for the area of 75 × 55 mm^2 by the high speed camera. The tracer particles are polymer fluorescence particles (DANTEC DYNAMICS) which contain Rhodamine B. The mean diameter, specific gravity and refractive index of the polymer fluorescence particles are respectively 10 μm, 1.50 g/cm^3 and 1.68. A sharp cut filter whose cut-off wavelength is 560 nm is applied in front of the camera lens. The seeding density is adjusted to obtain 10-15 particle pairs in each interrogation windows whose size is set to 32 × 32 pixels. The interrogation windows are overlapped 50% in each direction. Thus, the measurement sampling volume is 1.47(x) × 1.47(y) × 1.0(z) mm^3. The image sampling rate is adjusted depending on the averaged particle displacement during the time interval. In the present experiments, the averaged particle displacement is set to be about 25% length (6-8 pixels) of the interrogation window cell. To obtain the statistical data, at each location, 9000 image pairs are processed at each frame. After recording, obtained data are processed by commercial software (DANTEC DYNAMICS, Dynamic Studio 3.1) with the fast Fourier transform cross-correlation technique. Each image is processed to produce instantaneous 101 × 74 vectors.

2.3. Experimental conditions

The experimental parameter is the type of porous media. The flow Reynolds number is defined as $Re_{in}=U_{in}D_H/\nu$ where U_{in} is the inlet velocity, D_H is the hydraulic diameter of the clear flow region of the test section, ν is the kinematic viscosity of the fluid. The inlet velocity rate is measured using the digital flow meter (FD-MH10A, KEYENCE). The Reynolds number is set to Re_{in}=3600. The

measurement sections shown in figure 3 are seven *x*-*y* sections (i-vii) whose intervals are 2.5mm from the symmetry plane.

3. Results and discussions

3.1. Secondary flows

Figure 4 shows contour maps of streamwise and wall normal mean velocities in the cross-streamwise *z*-*y* planes for types A and B. The velocities are normalized by the inlet velocity U_{in}. The plane of z/H=0 corresponds to the symmetry plane of the test section duct, y/H=1.0 corresponds to the top wall, y/H=0 corresponds to the interface of the porous medium and y/H=-1.0 is the bottom wall. Here, the height of the clear flow region is H=50mm. Note that the white circles in figure 4 are the cross sections of the porous media. As can be seen in figure 4 (a) and (c), in the clear fluid region (y/H=0.0-1.0) the distribution of the streamwise velocities are skewed to the corners of the duct. It is because of the secondary flows driven by turbulence anisotropy. Such secondary flows are usually seen in rectangular ducts. To exclude the effects of such secondary flows from the discussions, it is chosen to use the data of sections i-vi which are near the symmetry plane.

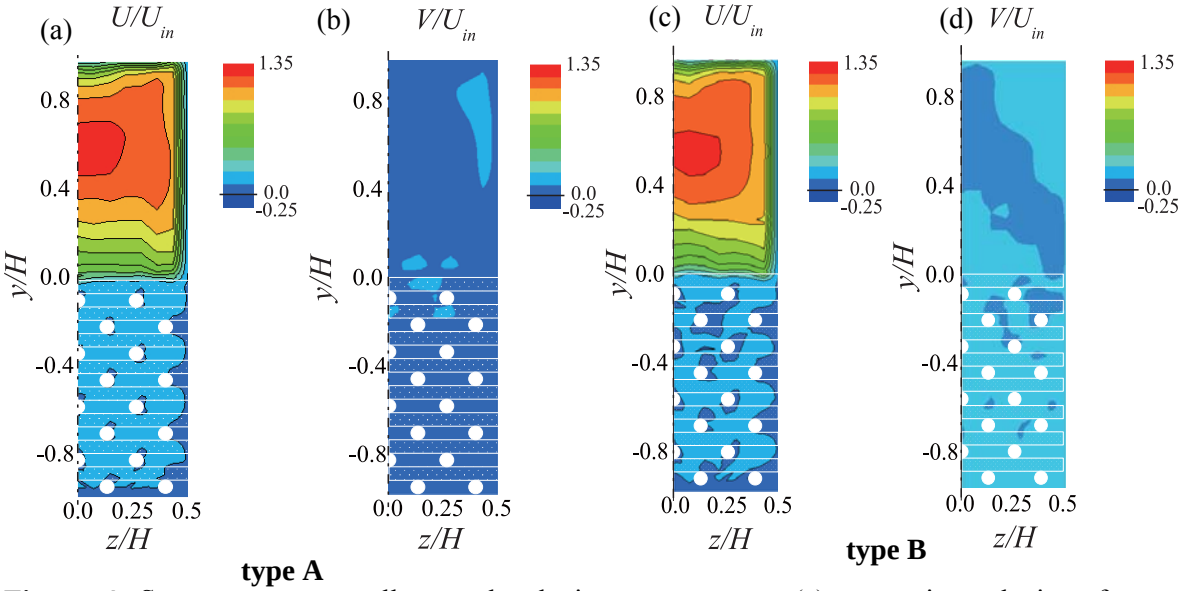

Figure 4. Streamwise and wall normal velocity contour maps;(a)streamwise velocity of type A, (b)wall normal velocity of type A, (c)streamwise velocity of type B, (d)wall normal velocity of type B.

3.2. Mean velocity profile

Figure 5 shows the streamwise and wall normal mean velocity profiles of the clear fluid regions (y/H=0.0-1.0) and inside the porous media (y/H=-1.0-0.0), respectively. These data are the time and spatial averaged values of sections i-vi of the fluid phase. The streamwise velocity U and the wall normal velocity V are normalized by the inlet velocity U_{in}. The red circle plots are the data of porous medium type A, and the blue square plots are the data of porous medium type B. Although the velocity profiles in the clear fluid region shown in figure 5 (a) and (b) do not show meaningful difference, as can be seen in figure 5 (c), the streamwise velocity in the porous medium type A is larger than that of type B. This is because the streamwise permeability K_x of type A is a little larger than that of type B. It is seen that the cross-streamwise velocity profiles in the porous media shown in figure 5 (d) are more affected by the local structure of the porous media.

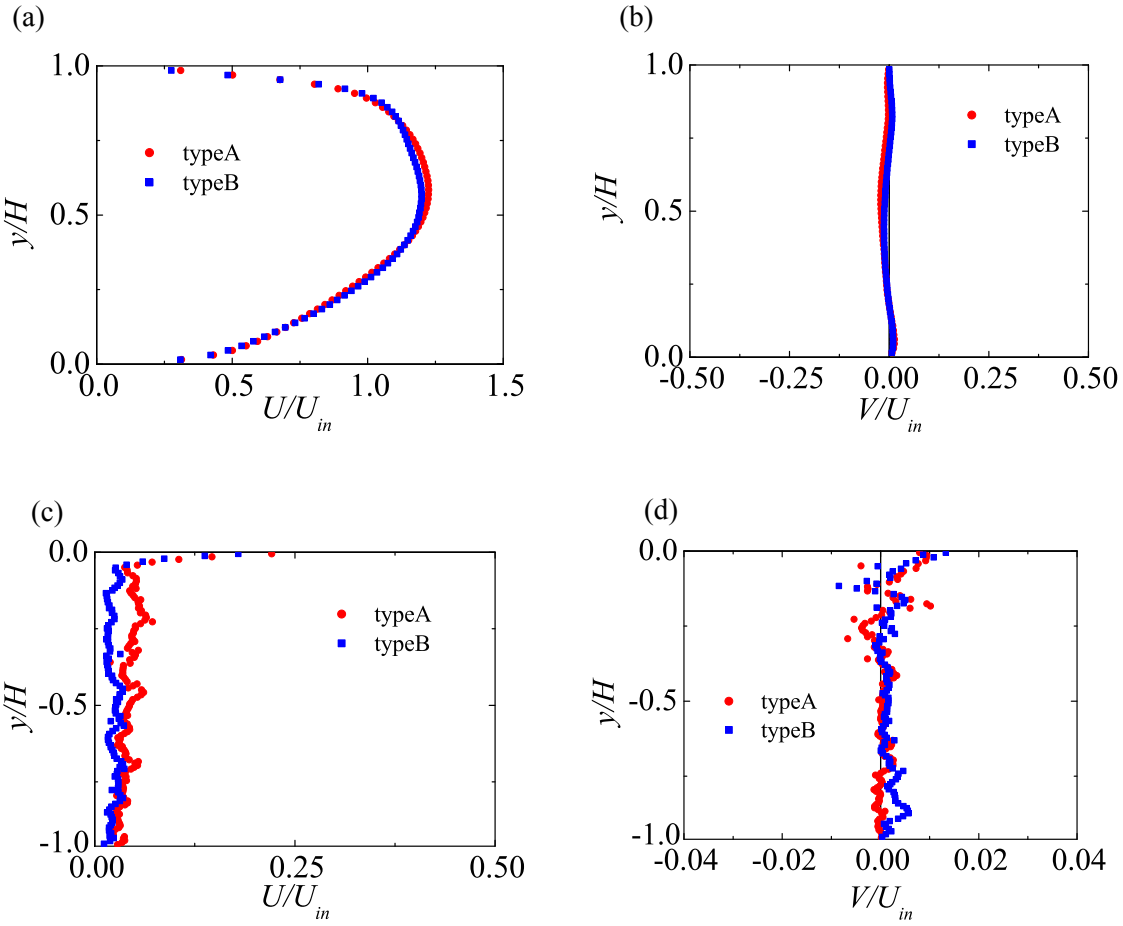

Figure 5. Streamwise and wall normal mean velocity profiles of the clear flow region and inside the porous media; (a) streamwise mean velocities in the clear flow region, (b)wall normal mean velocities in the clear flow region, (c)streamwise mean velocities inside the porous media, (d)wall normal mean velocities inside the porous media.

3.3. Fluctuation velocity and Reynolds shear stress

Figure 6 shows the RMS fluctuation velocity profiles in the clear flow regions and inside the porous media. Figure 7 shows the Reynolds shear stress profiles. As can be seen in figure 6 (a), (b) and (c), the RMS fluctuation velocities and $-\overline{u'v'}$ in the clear flow region of type A are larger than those of type B. Since the absolute value of the permeability $K(=\sqrt{K_x^2+K_y^2})$ for type A is larger than that for type B, turbulence over the porous medium type A becomes larger. This tendency is consistent with the previous study [1]. However, near the interface (y/H=0.0-0.1) the streamwise profile of type B is larger than that of type A. This is related with the tendency shown in figure 6 (c). The streamwise RMS fluctuation velocity of type B near the interface (y/H>-0.3) is clearly larger than that of type A, though it is not very clear in the wall normal components shown in figure 6 (d). It is considered that the mean pore diameter affects the turbulence significantly in the region under the interface since the eddies penetrating into the interface dissipate faster in the smaller pores. Indeed, the mean pore diameter of type B is clearly larger than that of type A as shown in table 1. Additionally, the difference of the streamwise RMS fluctuation velocities between type A and type B is larger than that of the wall normal RMS fluctuation velocities as observed in figure 6 (c) and (d). This is because, the difference in the major axis lengths of the spheroids which are circumscribed by the tubes composing the porous

media are larger than that in the minor axis lengths. Indeed, the major axis of spheroid of type A is 10mm, while that of type B is 13mm. However, the minor axes of spheroids of type A and B are both 9mm. Note that the major and minor axes are aligned with the streamwise and cross-streamwise directions, respectively.

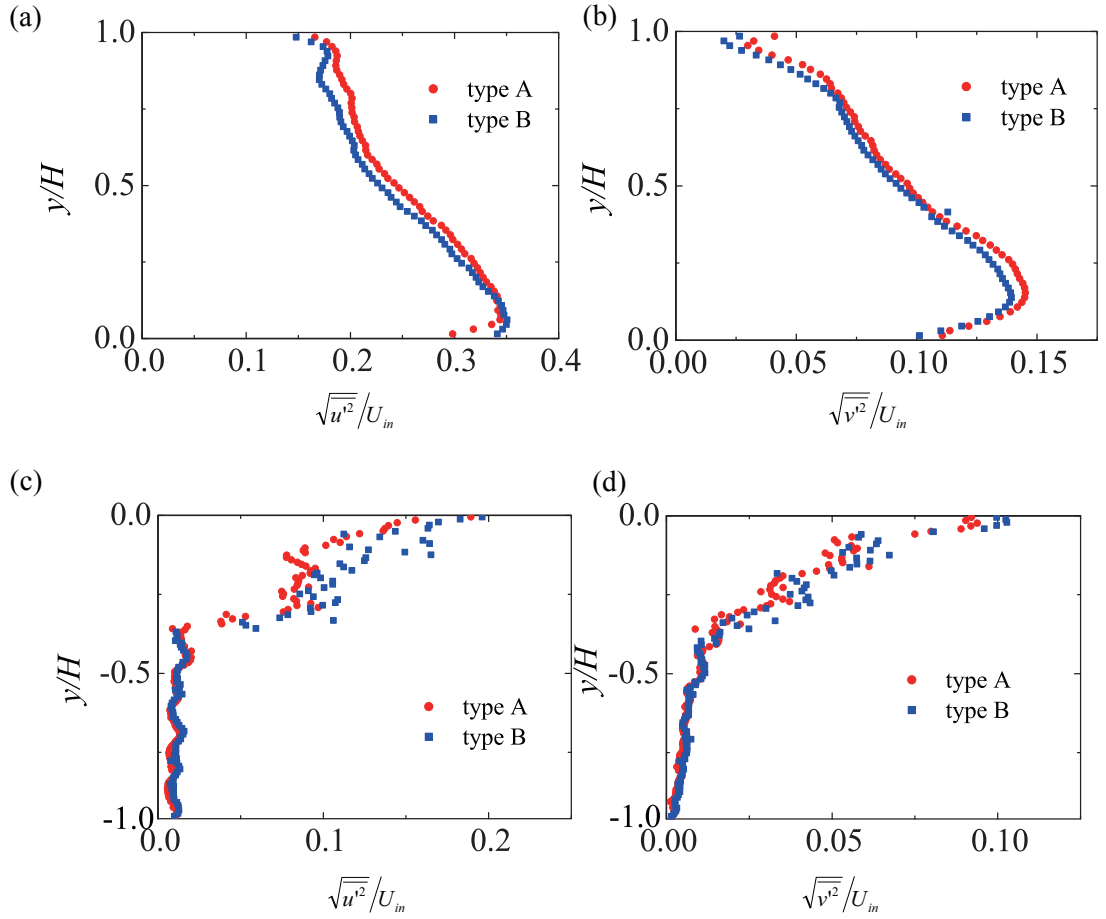

Figure 6. Streamwise and wall normal fluctuation velocity profiles of the clear flow region and inside the porous media; (a)streamwise fluctuation velocity in the clear flow region, (b)wall normal fluctuation velocity in the clear flow region, (c)streamwise fluctuation velocity inside the porous media, (d)wall normal fluctuation velocity inside the porous media.

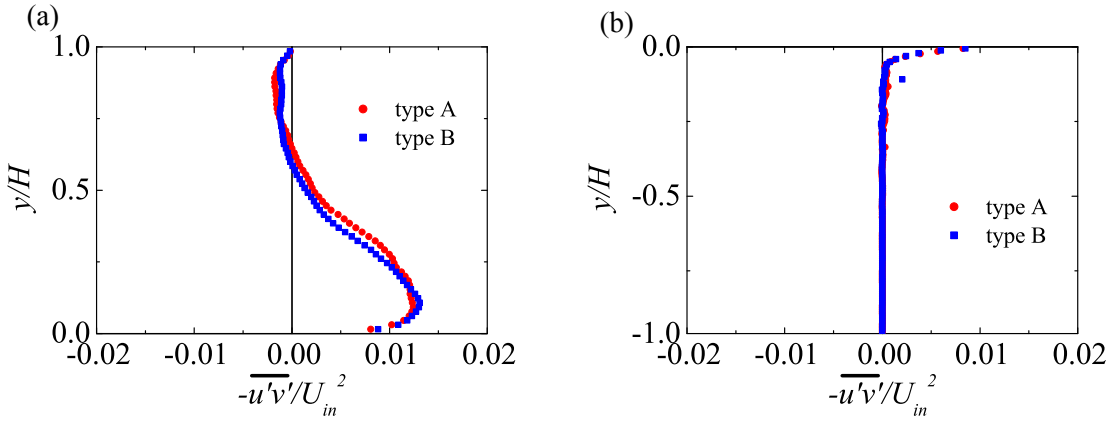

Figure 7. Reynolds shear stress profiles; (a)in the clear flow region, (b)inside the porous media.

4. Conclusions

Two velocity components of the turbulent fields over and inside hetero-porous media are measured by PIV with the refractive index matching method. A handmade porous medium is settled up to the bottom half of the channel height. Two kinds of heterogeneous porous media are applied to the present experiments to discuss the effect of the characteristics of the porous media. They have the same porosity but different permeabilities and mean pore diameters. It is found that the larger stream permeability leads to larger streamwise mean velocities inside the porous media whilst the larger mean pore diameter allows a higher level of turbulence near the interface. It is also confirmed that turbulence over the interface tends to be larger when the absolute value of the permeability becomes larger.

References

[1] Suga K, Matsumura Y, Ashitaka Y, Tominaga S and Kaneda M 2010 *Int.J. Heat Fluid Flow* **31** 974-984
[2] Suga K, Mori M and Kaneda M 2011 *Int.J. Heat Fluid Flow* **32** 586-595
[3] Suga K, Tominaga S, Mori M and Kaneda M 2013 *Flow Turbulence Combust.* **91** 19-40
[4] Suga K, Nishimura W, Yamamoto T and Kaneda M 2014 *Int.J. Hydrogen Energy* **39** 5942-5954